Heat Transfer Engineering
Publication details, including instructions for authors and subscription information:
http://www.tandfonline.com/loi/uhte20

Pressure- and Temperature-Driven Flow Through Triangular and Trapezoidal Microchannels

Konstantinos Ritos [a], Yiannis Lihnaropoulos [a], Stergios Naris [a] & Dimitris Valougeorgis [a]
[a] Department of Mechanical Engineering, University of Thessaly, Volos, Greece

Available online: 27 Jun 2011

To cite this article: Konstantinos Ritos, Yiannis Lihnaropoulos, Stergios Naris & Dimitris Valougeorgis (2011): Pressure- and Temperature-Driven Flow Through Triangular and Trapezoidal Microchannels, Heat Transfer Engineering, 32:13-14, 1101-1107

To link to this article: http://dx.doi.org/10.1080/01457632.2011.562455

Heat Transfer Engineering, 32(13–14):1101–1107, 2011

ISSN: 0145-7632 print / 1521-0537 online
DOI: 10.1080/01457632.2011.562455

Taylor & Francis
Taylor & Francis Group

Pressure- and Temperature-Driven Flow Through Triangular and Trapezoidal Microchannels

KONSTANTINOS RITOS, YIANNIS LIHNAROPOULOS, STERGIOS NARIS, and DIMITRIS VALOUGEORGIS

Department of Mechanical Engineering, University of Thessaly, Volos, Greece

A detailed study of pressure- and temperature-driven flows through long channels of triangular and trapezoidal cross sections is carried out. Due to the imposed pressure and temperature gradients there is a combined gas flow consisting of a thermal creep flow from the cold toward the hot reservoir and a Poiseuille flow from the high- toward the low-pressure reservoir. The formulation is based on the linearized Shakhov model subject to Maxwell boundary conditions, and it is solved numerically using a finite-difference scheme in the physical space and the discrete velocity method in the molecular velocity space. The results are valid in the whole range of the Knudsen number. In addition to the dimensionless flow rates, a methodology is presented to estimate for a certain set of input data the mass flow rates and the pressure distribution along the channel. Finally, special attention is given to the case of zero net mass flow and to the computation of the coefficient of the thermomolecular pressure difference.

INTRODUCTION

The fully developed flow of rarefied gases through long channels of various cross sections is of major importance in microfluidics [1]. Extensive theoretical and experimental work has been performed in the case of circular and rectangular cross sections [2–6], while the corresponding work with channels of other cross sections is quite limited. In addition, most of the existing work is focused on isothermal pressure-driven flows.

In the present work based on linearized kinetic theory a detailed study of pressure- and temperature-driven flows through long channels of isosceles triangular and trapezoidal cross sections is carried out. This type of cross section, with an acute angle of 54.74°, is very common in microchannels manufactured by chemical etching on silicon wafers [7, 8]. For both the isothermal and non-isothermal flows, in addition to the flow rates a methodology is presented to estimate the pressure drop along the channel as well as the coefficient of the thermomolecular pressure difference (TPD). The analysis and the results are valid in the whole range of the Knudsen number.

Address correspondence to Professor Dimitris Valougeorgis, Department of Mechanical Engineering, University of Thessaly, Leoforos Athinon, Pedion Areos 38334, Volos, Greece. E-mail: diva@mie.uth.gr

FLOW CONFIGURATION

Consider a long channel of length L and hydraulic diameter $D_h = 4\tilde{A}/\tilde{\Gamma}$, where $\tilde{A}$ is the area and $\tilde{\Gamma}$ the perimeter of the channel cross section, connecting two reservoirs maintained at pressures and temperatures (P_1, T_1) and (P_2, T_2), with $P_1 \leq P_2$ and $T_1 < T_2$. Due to the imposed pressure and temperature gradients there is a combined gas flow consisting of a thermal creep flow from the cold toward the hot reservoir and a Poiseuille flow from the high toward the low pressure reservoir. Special attention is given to the case of zero net mass flow [2].

By taking $D_h \ll L$ the flow is considered as fully developed, and then end effects may be ignored. Even more, at each cross section the pressure and the temperature are constant and vary only along the flow direction $\tilde{z}$, i.e., $P = P(\tilde{z})$ and $T = T(\tilde{z})$. The imposed dimensionless pressure and temperature gradients are written as

$$X_P = \frac{D_h}{P}\frac{dP}{d\tilde{z}} \quad \text{and} \quad X_T = \frac{D_h}{T}\frac{dT}{d\tilde{z}} \tag{1}$$

At this point it is important to note that under the assumption of $D_h \ll L$ the dimensionless pressure and temperature gradients are always much less than 1, i.e.,

$$X_P \approx \frac{D_h}{L}\frac{\Delta P}{P} << 1 \quad \text{and} \quad X_T \approx \frac{D_h}{L}\frac{\Delta T}{T} << 1 \tag{2}$$

independently of the magnitude of the pressure and temperature differences $\Delta P = P_2 - P_1$ and $\Delta T = T_2 - T_1$, respectively, between the two reservoirs. This remark is easily explained by noting that even at large pressure or temperature differences, the ratios $\Delta P/P$ and $\Delta T/T$ are at most of order of 1, while $D_h/L << 1$. Therefore, even at large pressure and temperature drops, the quantities X_P and X_T are used as small parameters to linearize the flow equations [9].

The basic parameter characterizing both the Poiseuille and thermal creep flows is the rarefaction parameter δ, defined by

$$\delta = \frac{D_h P}{\mu u} \approx \frac{1}{Kn} \tag{3}$$

where μ is the gas viscosity at temperature T, and $\upsilon = \sqrt{2RT}$, with $R = k/m$ denoting the gas constant (k is the Boltzmann constant and m the molecular mass), is the most probable molecular velocity. It is seen that δ is proportional to the inverse Knudsen number; i.e., $\delta = 0$ and $\delta \to \infty$ correspond to the free molecular and hydrodynamic limits, respectively.

This type of combined rarefied gas flow has been investigated for circular [9, 10] and rectangular [11] channels and more recently for ellipsoidal ones [12]. In the present work we extend this approach to the case of channels with isosceles triangular and trapezoidal cross sections, which have been investigated recently only for the case of pressure-driven flows [13, 14].

The two cross sections considered in this work are shown in Figure 1. In both cases, B and h denote the base and the height of the cross sections, while the acute angle ω is taken equal to 54.74°. This angle is chosen because it is very common in microchannels manufactured by a photolithographic process. In the trapezoidal cross section the small base is denoted by b. For the triangular cross section the acute angle ω is adequate to define the dimensionless coordinates of the three apexes. The four apexes of the trapezoidal cross section may be defined by ω and the ratio b/B. The dimensionless coordinates of the apexes may be readily deduced by noting that

$$\frac{B}{D_h} = \frac{2\frac{h}{B}\left(1+\frac{b}{B}\right)}{1+\frac{b}{B}+\frac{h}{B}\frac{2}{\sin\omega}} \tag{4}$$

and

$$\tan\omega = \frac{2\frac{h}{B}}{1-\frac{b}{B}} \tag{5}$$

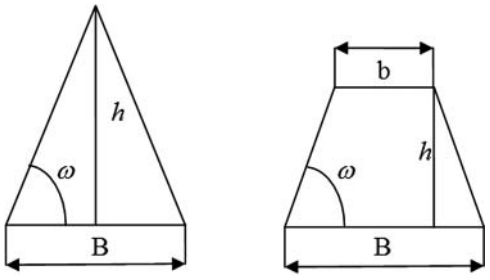

Figure 1 Triangular and trapezoidal cross sections.

Here, results are provided for the case of $b/B = 0$, which corresponds to the triangular cross section, and for two trapezoidal cross sections with $b/B = 0.5$ and 0.25. It is noted however, that the present analysis is general and may be applied to any cross section.

KINETIC FORMULATION

It has been shown, over the years, that in the case of non-isothermal flows driven by a temperature gradient, the linearized Shakov (S-model) kinetic equation [15] provides a reliable alternative of the Boltzmann equation, yielding accurate results with much less computational effort [2]. Following the well-known projection procedure, the linearized, dimensionless S-model equations modeling the present flow configuration may be written in the following form [12]:

$$\zeta\frac{\partial\Phi}{\partial s} + \delta\Phi = \delta\left[u_P + \frac{2}{15}q_P(\zeta^2-1)\right] - \frac{1}{2} \tag{6a}$$

$$\zeta\frac{\partial\Psi}{\partial s}\delta\Psi = \delta\frac{1}{5}q_P\zeta^2 - \frac{3}{4} \tag{6b}$$

Here, $\Phi = \Phi(x, y, \zeta, \theta)$ and $\Psi = \Psi(x, y, \zeta, \theta)$ are the unknown reduced distribution functions, (x, y) are the two components of the position vector, and (ζ, θ) are the magnitude and the polar angle of the molecular velocity vector, while

$$u_P(x, y) = \frac{1}{\pi}\int_0^\infty\int_0^{2\pi} \Phi e^{-\zeta^2}\zeta d\theta d\zeta \tag{7}$$

and

$$q_P(x, y) = \frac{1}{\pi}\int_0^\infty\int_0^{2\pi} \Psi e^{-\zeta^2}\zeta d\theta d\zeta + \frac{1}{\pi}\int_0^\infty\int_0^{2\pi} \times(\zeta^2-1)\Psi e^{-\zeta^2}\zeta d\theta d\zeta \tag{8}$$

are the bulk velocity and heat flux, respectively, in the flow direction. Also, s denotes the direction along the characteristic defined by the polar angle θ of the molecular velocity vector at some point (x, y). The associated linearized diffuse Maxwell boundary conditions are $\Phi^+ = 0$ and $\Psi^+ = 0$, where the plus sign refers to distributions representing particles departing from the walls.

Once the kinetic equations are solved, the macroscopic profiles are computed. Then the dimensionless flow rates for the pressure and temperature driven flows may be computed according to

$$G_P = \frac{2}{A}\iint_A u_p dA \tag{9}$$

and

$$G_T = \frac{2}{A}\iint_A q_p dA \tag{10}$$

respectively, where $A = \tilde{A}/D_h^2$ is the dimensionless cross section. It is noted that the well-known Onsager–Casimir relations have been used to obtain G_T [2, 12]. The flow rates G_P and G_T depend on the rarefaction parameter δ and the cross section A. The mass flow rate is given by

$$\dot{M} = \iint_{\tilde{A}} \rho u d\tilde{A} = G\frac{P\tilde{A}}{\upsilon} \tag{11}$$

where $\rho = \rho(z) = 2P(z)/\upsilon^2$, with $z = \tilde{z}/D_h$, is the mass density, u is the velocity profile of the overall flow, and

$$G = -X_P G_P + X_T G_T \tag{12}$$

is the combined dimensionless flow rate. Both G_P and G_T have been introduced so as to be always positive.

DIMENSIONLESS FLOW RATES G_P AND G_T

The system of the kinetic equations (6) has been solved by the discrete velocity method following a methodology recently introduced [13]. Numerical results for the dimensionless flow rates G_P and G_T are presented in Figures 2 and 3, respectively, for the three cross sections under consideration, with $10^{-3} \leq \delta \leq 10^2$.

It is seen that in both figures the results for the three cross sections are almost identical. This is due to the fact that the hydraulic diameter has been implemented as a characteristic length to nondimensionalize the problem. Any differences between the results are due to the approximation introduced to the concept of D_h and to its deviation from the exact hydraulic diameter. Both G_P and G_T follow the expected behavior in terms of δ. In particular, G_P is almost constant in highly rarefied atmospheres and proportional to δ in dense atmospheres, while the Knudsen minimum appears at about $\delta = 1$. Also, G_T is decreased monotonically as δ is increased and finally for $\delta > 10^2$ becomes negligibly small.

GENERALIZATION OF THE KINETIC SOLUTION TO LARGE PRESSURE AND TEMPERATURE DROPS

The solution of the S-model kinetic equations is obtained under the assumption of condition (2). When the pressure and temperature gradients are small, we may assume linear distributions along the channel and write

$$X_P \approx \frac{D_h}{L}\frac{\Delta P}{P_{av}} \quad \text{and} \quad X_T \approx \frac{D_h}{L}\frac{\Delta T}{T_{av}} \tag{13}$$

where $P_{av} = (P_1 + P_2)/2$ and $T_{av} = (T_1 + T_2)/2$. Then, for a certain type of gas flowing through a channel with specific geometry with given pressure and temperature (P_1, T_1) and (P_2, T_2), the mass flow rate may be computed using Eqs. (11), (12), and (13) as well as the dimensionless flow rates from Figures 2 and 3, using P_{av} as the reference pressure and δ_{av} as the corresponding rarefaction parameter.

However, when the pressure and temperature drops are large, the pressure distribution along the channel is not linear. Also, δ varies significantly along the channel. It depends on the local pressure and temperature according to

$$\delta(P, T) = \delta_1 \frac{P(z)}{P_1}\frac{T_1}{T(z)} \tag{14}$$

where $P(z)$ is unknown, while $T(z)$ is given ($z = \tilde{z}/D_h$). In this case, we introduce for the mass flow rate the complimentary expression

$$\dot{M} = G^* \frac{\tilde{A}P_1}{\upsilon_1}\frac{D_h}{L} \tag{15}$$

where G^* is an arbitrary unknown parameter, which, unlike the combined flow rate G in Eq. (12), does not depend on the local rarefaction parameter $\delta(z)$. From Eqs. (11) and (15), using Eqs. (1) and (12) we obtain the following ordinary differential equation for the pressure distribution:

$$G^* \frac{P_1}{P}\sqrt{\frac{T}{T_1}}\frac{D_h}{L} = -\frac{1}{P}\frac{dP}{dz}G_P + \frac{1}{T}\frac{dT}{dz}G_T \tag{16}$$

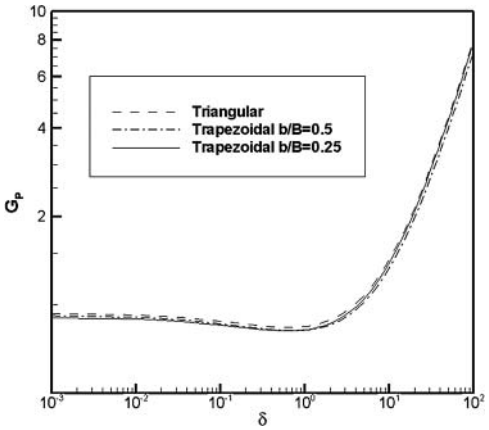

Figure 2 Dimensionless flow rate due to pressure drop in the whole range of δ.

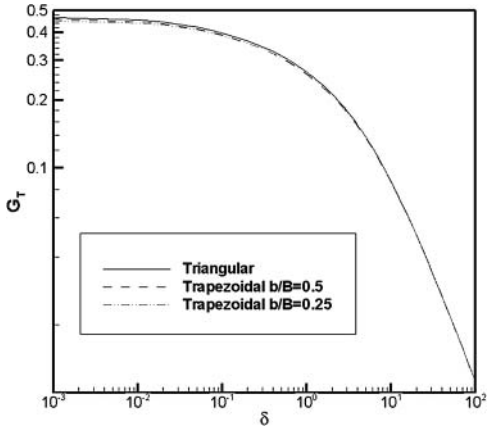

Figure 3 Dimensionless flow rate due to temperature drop in the whole range of δ.

It is mentioned again that the temperature distribution $T(z)$ along the channels is known. It is convenient to introduce the axial independent variable $z' = z/(L/D_h)$ and rewrite Eq. (16) in the form

$$\frac{1}{P_1}\frac{dP}{dz'} = \frac{P(z')}{P_1}\frac{1}{T}\frac{dT}{dz'}\frac{G_T}{G_P} - \frac{G^*}{G_P}\sqrt{\frac{T}{T_1}} \tag{17}$$

with $0 \le z' \le 1$. Equation (17) is solved for the unknown pressure distribution having G^* as a free parameter. In particular, introducing an initial guess for G^*, Eq. (17) is numerically integrated along z' starting with the initial condition $P(0) = P_1$. Then at the end of the integration path the estimated pressure $P(1)$ is compared to the known pressure P_2. If they do not match, the parameter G is accordingly updated and the whole process is repeated until the imposed convergence criteria between $P(1)$ and P_2 is satisfied. Upon convergence, in addition to the pressure distribution, the free parameter G^* has been adjusted. Finally, the mass flow rate may be computed from Eq. (15) provided that the cross section and the type of gas have been specified.

Indicatively, the parameter G^* for one temperature ratio $T_2/T_1 = 3.8$ and two pressure ratios $P_2/P_1 = 1$ and $P_2/P_1 = 10$ is given in Table 1 in terms of δ_1, which is taken as a reference rarefaction parameter. The ratio $T_2/T_1 = 3.8$ corresponds to a situation where one reservoir is maintained at liquid nitrogen temperature, while the other one is maintained at the room temperature. For $P_2/P_1 = 1$ the flow is driven only by the temperature gradient from the cold reservoir toward the hot one (parameter G^* and therefore $\dot{M}$ are positive). As expected, G^* is decreased as δ_1 is increased. For $P_2/P_1 = 10$ the values of the parameter G^* are quite different. In this case there is a combined flow and due to the large pressure ratio the pressure-driven flow dominates over the temperature-driven flow. The parameters G^* and therefore $\dot{M}$ are negative, indicating clearly that the gas flows from the hot reservoir, where the pressure is higher, to the cold one, where the pressure is lower. As expected, in this case G^* is increased as δ_1 is increased.

Next, in Figure 4, the pressure distribution along the trapezoidal channel, with $b/B = 0.25$, $P_2/P_1 = 1$, and $T_2/T_1 = 3.8$, is shown for various rarefaction parameters δ_1. It is interesting to note that even though $P_1 = P_2$, there is an increase of the pressure inside the channel, which becomes larger as the atmosphere becomes more rarefied. Actually, for $\delta = 30$ the pressure increase is negligible small, while for $\delta = 0.01$ the maximum increase is about 17% with respect to the pressure of the reservoirs.

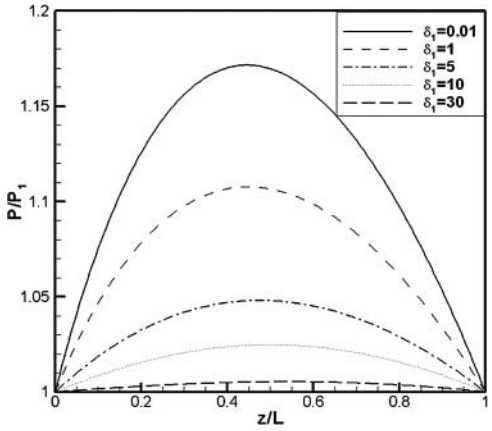

Figure 4 Pressure distribution along a trapezoidal channel, with $b/B = 0.25$ and $P_2/P_1 = 1$.

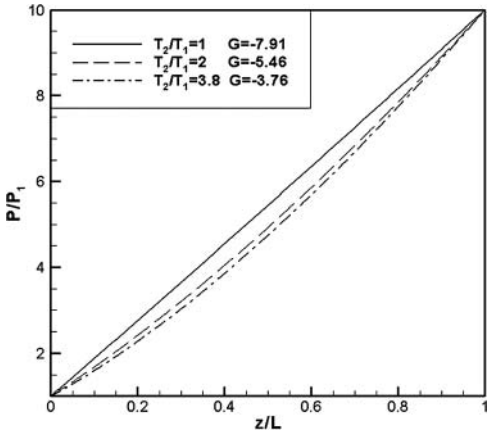

Figure 5 Pressure distribution along a trapezoidal channel, with $b/B = 0.25$, for $P_2/P_1 = 10$ and $\delta_1 = 0.01$.

Pressure distributions along the trapezoidal channel, with $b/B = 0.25$ and $P_2/P_1 = 10$ are also shown in Figures 5, 6, and 7 for $\delta_1 = 0.01$, 1, and 10, respectively. In each figure three temperature ratios, namely, $T_2/T_1 = 1$, 2, and 3.8, are considered. The pressure distributions for $T_2/T_1 = 1$ correspond to the pure pressure-driven flow and they agree qualitatively with the corresponding ones obtained in [14]. They are linear for small values of δ_1 and then, as δ_1 is increased, they become parabolic. The corresponding profiles for the cases of combined flow with $T_2/T_1 = 2$ and 3.8 are also presented. The deviation between the pressure profiles along the channel for the isothermal and non-isothermal flow is clearly demonstrated. The presented results may be considered as typical for other pressure and temperature

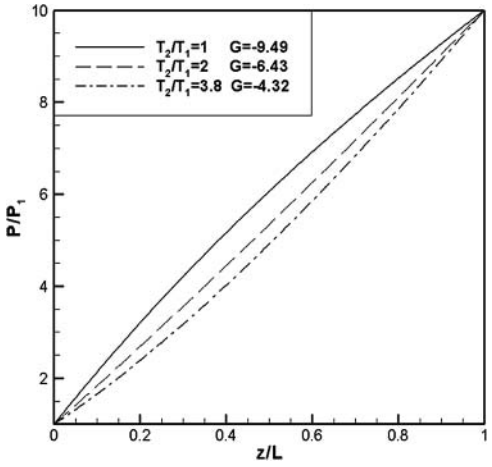

Figure 6 Pressure distribution along a trapezoidal channel, with $b/B = 0.25$, for $P_2/P_1 = 10$ and $\delta_1 = 1$.

Table 1 Parameter G^* for $P_2/P_1 = 1$ and $P_2/P_1 = 10$, with $T_2/T_1 = 3.8$

	G^*					
δ_1	Triangular	Trapezoidal $b/B = 0.5$; $P_2/P_1 = 1 T_2/T_1 = 3.8$	Trapezoidal $b/B = 0.25$	Triangular	Trapezoidal $b/B = 0.5$ $P_2/P_1 = 10$; $T_2/T_1 = 3.8$	Trapezoidal $b/B = 0.25$
0.01	0.4492	0.4417	0.4357	–3.83	–3.76	–3.71
0.1	0.4065	0.3990	0.3955	–3.77	–3.70	–3.66
0.5	0.3341	0.3270	0.3268	–4.04	–3.92	–3.92
1	0.2898	0.2834	0.2846	–4.50	–4.32	–4.36
5	0.1681	0.1650	0.1669	–8.29	–7.73	–8.06
10	0.1164	0.1151	0.1162	–13.01	–12.02	–12.68
30	0.0539	0.0538	0.0540	–31.83	–29.10	–31.05

ratios. Also, similar behavior has been observed for the other two cross sections studied in the present work.

THERMOMOLECULAR PRESSURE DIFFERENCE

An interesting situation exists when the pressure- and temperature-driven flows counterbalance each other and the net flow between the reservoirs is equal to zero [2, 12]. This situation is known as the thermomolecular pressure difference (TPD) state and the relation between P_1, P_2, T_1, and T_2 can be written in the form

$$P_2/P_1 = (T_2/T_1)^{\gamma} \tag{18}$$

where the TPD coefficient γ depends on the gas rarefaction, the pipe geometry, and the type of the gas, as well as on the gas–surface interaction. The last of these is not considered in the present work since we have assumed purely diffuse reflection at the walls. Our objective here is to develop a procedure for the estimation of the coefficient γ provided that all required data are given.

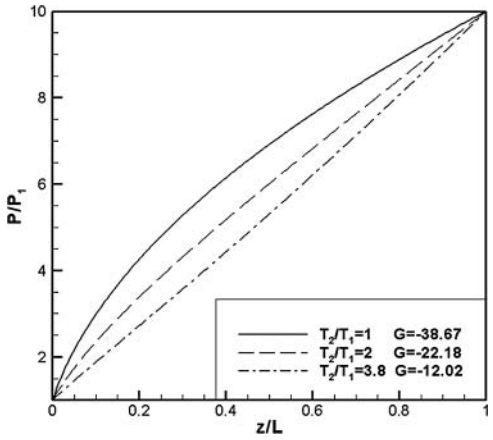

Figure 7 Pressure distribution along a trapezoidal channel, with $b/B = 0.25$, for $P_2/P_1 = 10$ and $\delta_1 = 10$.

By setting, in Eq. (16), $G^* = 0$, we find

$$\frac{1}{P}\frac{dP}{dz}G_P = \frac{1}{T}\frac{dT}{dz}G_T \tag{19}$$

Next, the dimensionless pressure and temperature are introduced as

$$p = P/P_1 \qquad \text{and} \qquad \tau = T/T_1 \tag{20}$$

Based on the preceding, the rarefaction parameter in any cross section, given in Eq. (14), may be expressed as

$$\delta(p, \tau) = \delta_1 \frac{p}{\tau}. \tag{21}$$

Then, Eq. (19) reads

$$\frac{dp}{d\tau} = \frac{p}{\tau}\frac{G_T(\delta_1 p/\tau)}{G_P(\delta_1 p/\tau)} \tag{22}$$

Equation (22) is an ordinary differential equation where p and τ are the dependent and independent variables respectively, i.e., $p = p(\tau)$, with the initial condition $p = 1$ at $\tau = 1$. By integrating Eq. (22) along $1 \le \tau \le T_2/T_1$ the unknown pressure P_2/P_1 is found. In this case no iteration is needed, since $p(\tau)$ depends only on the ratio T_2/T_1 and on the rarefaction parameter δ_1. The quantities G_P and G_T along the integration path are computed from the kinetic solution using the corresponding estimates of δ. Finally, the coefficient γ is calculated from Eq. (18) as

$$\gamma = \frac{\ln(P_2/P_1)}{\ln(T_2/T_1)}. \tag{23}$$

This procedure has been applied, mainly for demonstration purposes, to the three cross sections under investigation for $T_2/T_1 = 3.8$ and a wide range of δ_1. Results for γ are presented in Table 2, where in addition to the triangular and trapezoidal cross sections results are included for comparison purposes for a square and an orthogonal channel with aspect ratio $b/B = 0.05$. It is clearly seen that the coefficient γ depends strongly on the reference rarefaction parameter. As δ_1 is increased, γ is decreased. This is easily explained, since as the atmosphere becomes more dense the thermal creep flow is decreased and therefore larger temperature drops are needed to maintain the

Table 2 TPD coefficient γ over a wide range of δ_1 for various cross sections

	γ				
δ_1	Triangular	Trapezoidal $b/B = 0.5$	Trapezoidal $b/B = 0.25$	Square	Rectangular $b/B = 0.05$
0.01	0.4956	0.4955	0.4958	0.4951	0.4780
0.02	0.4908	0.4907	0.4912	0.4908	0.4628
0.05	0.4793	0.4791	0.4800	0.4809	0.4362
0.1	0.4648	0.4646	0.4659	0.4684	0.4089
0.2	0.4444	0.4441	0.4459	0.4500	0.3782
0.5	0.4018	0.4019	0.4043	0.4106	0.3274
0.8	0.3717	0.3722	0.3747	0.3822	0.2971
1	0.3552	0.3560	0.3584	0.3664	0.2813
2	0.2940	0.2961	0.2978	0.3068	0.2255
5	0.1953	0.1991	0.1991	0.2072	0.1405
10	0.1204	0.1246	0.1233	0.1290	0.08068
20	0.06120	0.06467	0.06290	0.06587	0.03750
30	0.03734	0.03987	0.03840	0.04020	0.02166
50	0.01814	0.01957	0.01866	0.01951	0.009891
80	0.008572	0.009315	0.008810	0.009227	0.004485
100	0.005871	0.006396	0.006032	0.006332	0.003037

no net flow condition. On the contrary, in highly rarefied atmospheres the effect of the thermal creep flow is significant and larger pressure drops are needed to counter balance this flow. The coefficient γ depends also on the geometry of the cross section.

CONCLUDING REMARKS

The pressure- and temperature-driven flows through channels of triangular and trapezoidal cross sections have been investigated. The flow is simulated by the linearized Shakhov kinetic model subject to Maxwell boundary conditions. The governing integrodifferential equations are solved numerically by the discrete velocity method. Numerical results are presented for the dimensionless flow rates in the whole range of the rarefaction parameter. Also, a procedure for estimating the pressure distribution along the channels and the coefficient of the thermomolecular pressure difference has been presented. Results for certain pressure and temperature drops have been reported.

It is hoped that the presented analysis and results may be useful for comparisons with experimental work, as well as to the design and optimization of micro-devices. The implemented methodology may be easily applied to channels of other cross sections provided that the channel is sufficiently long ($D_h \ll L$) and the corresponding kinetic solution is available. The type of gas–surface interaction can be also included by considering diffuse–specular reflection at the walls.

NOMENCLATURE

A dimensionless cross section area
$\tilde{A}$ cross section area (m^2)
B base length of the cross section (m)
b small base length of the trapezoidal cross section (m)
D_h hydraulic diameter (m)
G dimensionless flow rate
G^* free parameter
h height of the cross section (m)
k Boltzmann's constant (J/K)
Kn Knudsen number
L channel length (m)
$\dot{M}$ mass flow rate (kg/s)
m molecular mass (kg/mol)
P pressure (N/ m^2)
p dimensionless pressure
q dimensionless heat flux
R gas constant (J/K-kg)
T temperature (K)
u dimensionless bulk velocity (m/s)
X_P dimensionless pressure gradient
X_T dimensionless temperature gradient
x,y,z dimensionless coordinates

Greek Symbols

$\tilde{\Gamma}$ perimeter of the cross section (m)
γ TPD coefficient
ΔP pressure difference (N-t/m^2)
ΔT temperature difference (K)
δ rarefaction parameter
ζ magnitude of the dimensionless molecular velocity vector
θ polar angle of the dimensionless molecular velocity vector
τ dimensionless temperature
μ viscosity (kg/s-m)
ρ density (kg/m^3)
υ most probable molecular velocity (m/s)
Φ reduced distribution function

Ψ reduced distribution function
ω acute angle (°)

REFERENCES

[1] Kandlikar, S. G., and Garimella, S., *Heat Transfer and Fluid Flow in Minichannels and Microchannels*, Elsevier, Oxford, 2006.

[2] Sharipov, F., and Seleznev, V., Data on Internal Rarefied Gas Flows, *Journal of Physical and Chemical Reference Data*, vol. 27, pp. 657–706, 1998.

[3] Colin, S., and Lalonde, P., Validation of a Second-Order Slip Flow Model in Rectangular Microchannels, *Heat Transfer Engineering*, vol. 25, no. 3, pp. 23–30, 2004.

[4] Lockerby, D. A., and Reese, J. M., On the Modelling of Isothermal Gas Flows at the Microscale, *Journal of Fluid Mechanics*, vol. 604, pp. 235–261, 2008.

[5] Tang, G. H., Zhang, Y. H., and Emerson, D. R., Lattice Boltzmann Models for Nonequilibrium Gas Flows, *Physical Review*, vol. E 77, pp. 046701.1–6, 2008.

[6] Pitakarnnop, J., Varoutis, S., Valougeorgis, D., Geoffroy, S., Baldas, L., and Colin, S., A Novel Experimental Setup for Gas Microflows, *Microfluid Nanofluid*, vol. 8, pp. 57–72, 2010.

[7] Morini, G. L., Spiga, M., and Tartarini, P., The Rarefaction Effect on the Friction Factor of Gas Flow in Microchannels, *Superlattices and Microstructures*, vol. 35, pp. 587–599, 2004.

[8] Pitakarnnop, J., Geoffroy, S., Colin, S., and Baldas, L., Slip Flow in Triangular and Trapezoidal Microchannels, *International Journal of Heat and Technology*, vol. 26, no. 1, pp. 167–174, 2008.

[9] Sharipov, F., and Seleznev, V., Rarefied Gas Flow Through a Long Tube at Any Pressure Ratio, *Journal of Vacuum Science & Technology A*, vol. 12, no. 5, pp. 2933–2935, 1994.

[10] Sharipov, F., Rarefied Gas Flow Through a Long Tube at Any Temperature Ratio, *Journal of Vacuum Science & Technology A*, vol. 14, no. 4, pp. 2627–2635, 1996.

[11] Sharipov, F., Non-Isothermal Gas Flow Through Rectangular Microchannels, *Journal of Micromechanics and Microengineering*, vol. 9, pp. 394–401, 1999.

[12] Graur, I., and Sharipov, F., Non-Isothermal Flow of a Rarefied Gas Through a Long Pipe With Elliptic Cross Section, *Microfluidics and Nanofluidics*, vol. 6, pp. 267–275, 2009.

[13] Naris, S., and Valougeorgis, D., Rarefied Gas Flow in a Triangular Duct Based on a Boundary Fitted Lattice, *European Journal of Mechanics B/Fluids*, vol. 27, pp. 810–822, 2008.

[14] Varoutis, S., Naris, S., Hauer, V., Day, C., and Valougeorgis, D., Computational and Experimental Investigation of Gas Flows Through Long Channels of Various Cross Sections in the Whole Range of the Knudsen Number, *Journal of Vacuum Science & Technology A*, vol. 27, no. 1, pp. 89–100, 2009.

[15] Shakhov, E. M., Generalization of the Krook Equation, *Fluid Dynamics*, vol. 3, pp. 142–145, 1968.

Konstantinos Ritos is a doctoral student at the Mechanical Engineering Department in University of Strathclyde. He obtained a diploma in mechanical engineering from the University of Thessaly (Greece) in 2009. His research is focused on computational micro and nano fluidics.

Yannis Lihnaropoulos is a Ph.D. student at the Mechanical Engineering Department of the University of Thessaly (Greece). He obtained a B.Sc. in mathematics from University of Ioannina (Greece) in 1992 and a postgraduate diploma in mechanical engineering from the University of Thessaly in 2008. He is currently involved with research in rarefied gas flows and kinetic theory.

Steryios Naris holds visiting positions in the Technological Educational Institute of Larisa and in the Department of Mechanical Engineering of the University of Thessaly. He has a degree in mechanical engineering from the Aristotle University Thessaloniki (1998) and M.Sc. (2003) and Ph.D. in microfluidics (2005) from the University of Thessaly. His work is focused on the numerical simulation of nonequilibrium flows. He has 14 journal and more than 35 conference proceedings publications.

Dimitris Valougeorgis is a professor in the Department of Mechanical Engineering of the University of Thessaly in Volos, Greece. He obtained a diploma in mechanical engineering from the Aristotelion University of Thessaloniki, Greece in 1980 and an M.S. and a Ph.D. degree in mechanical engineering from the Virginia Polytechnic Institute and State University in 1982 and 1985, respectively. His research is in kinetic theory of gases, rarefied gas dynamics, and nonequilibrium transport phenomena. He has published about 45 articles in journals and more than 100 articles in proceedings of conferences.